

## Electronic structure of possible 3d 'heavy-fermion' compound $\text{Fe}_2\text{VAI}$

This article has been downloaded from IOPscience. Please scroll down to see the full text article.

1998 J. Phys.: Condens. Matter 10 L119

(<http://iopscience.iop.org/0953-8984/10/8/002>)

View [the table of contents for this issue](#), or go to the [journal homepage](#) for more

Download details:

IP Address: 171.66.16.209

The article was downloaded on 14/05/2010 at 12:19

Please note that [terms and conditions apply](#).

## LETTER TO THE EDITOR

**Electronic structure of possible 3d ‘heavy-fermion’  
compound Fe<sub>2</sub>VAl**G Y Guo<sup>†</sup>, G A Botton<sup>‡</sup> and Y Nishino<sup>||</sup><sup>†</sup> Daresbury Laboratory, Warrington, Cheshire WA4 4AD, UK<sup>‡</sup> Materials Science and Metallurgy Department, University of Cambridge, Cambridge CB2 3QZ, UK<sup>||</sup> Materials Science and Engineering Department, Nagoya Institute of Technology, Nagoya 466, Japan

Received 3 November 1997

**Abstract.** Recent transport, specific heat and magnetization measurements indicated that the Heusler-type Fe<sub>2</sub>VAl compound is a candidate for a 3d heavy-fermion system. As a first step towards a detailed theoretical understanding of the observed anomalous electronic properties of this compound, we have performed first-principles electronic structure and total energy calculations for Fe<sub>3</sub>Al and Fe<sub>2</sub>VAl. The calculated lattice constants and magnetic moments are in good agreement with experiments. Remarkably, we find that, unlike Fe<sub>3</sub>Al, Heusler-type Fe<sub>2</sub>VAl is a nonmagnetic semimetal with a narrow pseudogap at the Fermi level. Furthermore, our calculations suggest that the observed large enhancement of electronic specific heat coefficient is largely caused by the mechanisms such as spin-fluctuations rather than electron–phonon coupling in Fe<sub>2</sub>VAl. The relations between the existence of the Fermi surface and negative temperature dependence of the low-temperature electrical resistivity in Fe<sub>2</sub>VAl are discussed and further experimental and theoretical work is suggested.

Intermetallic compound Fe<sub>3</sub>Al is a ferromagnet with a  $D0_3$  crystal structure (see figure 1). Recently, Nishino *et al* found an anomalous temperature dependence of electrical resistivity in a series of pseudobinary alloys (Fe<sub>1-x</sub>V<sub>x</sub>)<sub>3</sub>Al in which some Fe atoms in the parent compound Fe<sub>3</sub>Al are replaced by V atoms [1]. A single phase of the  $D0_3$  structure remains stable over a wide range of V composition. In particular, the Heusler-type Fe<sub>2</sub>VAl compound ( $x = 0.33$ ) exhibits a resistivity anomaly in a manner similar to a narrow-gap semiconductor. Furthermore, electronic specific heat measurements revealed a large mass enhancement [1], suggesting that Fe<sub>2</sub>VAl is a possible candidate for a 3d heavy-fermion system.

In this letter, in order to gain insight into these fascinating properties of the Heusler-type Fe<sub>2</sub>VAl, we present the first *ab initio* electronic structure and total energy calculations for Fe<sub>2</sub>VAl. For comparison, we have also performed the same calculations for Fe<sub>3</sub>Al. We find that unlike Fe<sub>3</sub>Al, Heusler-type Fe<sub>2</sub>VAl is a nonmagnetic semimetal. There is a sharp pseudogap in the density of states spectrum at the Fermi level. The results of the present calculations explain some of the previous electronic and magnetic measurements [1].

Fe<sub>3</sub>Al crystallizes in a face-centred cubic (fcc) structure ( $D0_3$ ) (see figure 1). There are three Fe atoms per unit cell belonging to two different types. The first type consisting of one Fe atom (denoted by Fe(I)) in the unit cell, is surrounded by eight Fe atoms in an octahedral coordination and the second type consisting of two Fe atoms (denoted by Fe(II)) in the unit cell, is surrounded by four Al and four Fe atoms in a tetrahedral coordination. When Fe(I) is replaced by V, the resultant structure is a Heusler-type compound (denoted

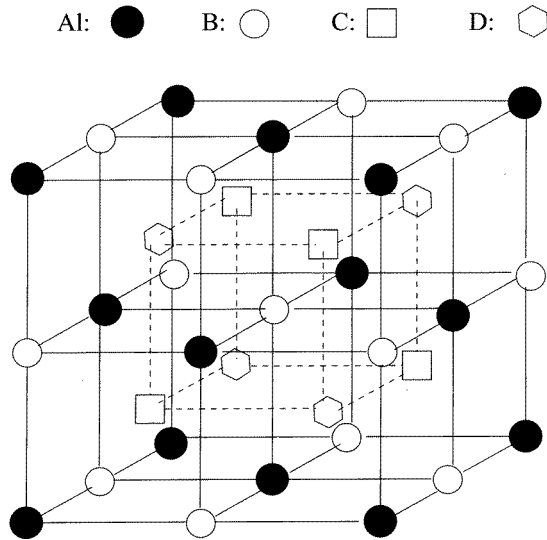


**Figure 1.** Unit cell of four interpenetrating fcc sublattices showing the four types of site at Al (000), B (1/2, 1/2, 1/2), C (1/4, 1/4, 1/4), D (3/4, 3/4, 3/4). Structures:  $DO_3$   $Fe_3Al$ , B = Fe(I), C = D = Fe(II);  $L2_1$   $Fe_2VAl$ , B = V, C = D = Fe;  $FeVFeAl$  (see text), B = Fe, C = V, D = Fe.

here by  $Fe_2VAl$ ) with the cubic  $L2_1$  lattice (see figure 1). Both the  $DO_3$  and  $L2_1$  structures have the same full cubic symmetry. However, if one of the Fe(II) atoms is substituted by V, the resultant structure no longer has the inversion symmetry although it is still a cubic lattice. We denote this structure  $FeVFeAl$ .

We first performed all-electron self-consistent spin-polarized electronic structure and total energy calculations for all three systems by using the linear muffin-tin orbital (LMTO) method [2]. These calculations are based on the first-principles density functional theory with the standard local spin-density approximation (LSDA) [3, 4]. The most accurate local exchange–correlation potential parametrized by Vosko *et al* [5] was used throughout. The core electrons were treated fully relativistically by solving the Dirac equation but the valence electrons were treated only scalar-relativistically [6]. The basis functions used were s, p and d MTOs. The calculations were carried out for several lattice constants starting from the experimental value ( $a = 10.866$  au) for  $Fe_2VAl$ . The atomic sphere radius ratio used is 2.859 (Al):2.615 (Fe):2.615 (V). The number of  $k$ -points in the irreducible Brillouin zone wedge used in the analytic tetrahedron BZ integration [7] is 240.

Our spin-polarized electronic structure calculations show that  $Fe_3Al$  is a ferromagnet (or strictly speaking, a ferrimagnet) and  $Fe_2VAl$  is nonmagnetic. Interestingly,  $FeVFeAl$  is also a ferromagnet (or a ferrimagnet), suggesting the crucial role played by the Fe(I) in the magnetization in the  $(Fe_{1-x}V_x)_3Al$  alloys. The calculated total energy as a function of lattice constant is plotted in figure 2 for ferromagnetic  $Fe_3Al$  and  $FeVFeAl$  as well as nonmagnetic  $Fe_2VAl$ . Note that no magnetic state can be stabilized for  $Fe_2VAl$  in the range of the lattice constant shown in figure 2. This shows that the observed magnetization in  $(Fe_{1-x}V_x)_3Al$  ( $x < 0.3$ ) [8, 1] is caused by the larger Fe concentration especially the occupation of the Fe(I) sites by the Fe atoms rather than by the larger lattice constant in these alloys. The theoretical lattice constant and bulk modulus for these systems were then obtained by fitting the calculated total energies to the equation of state of Murnaghan [9]. The calculated

lattice constants and other properties at these theoretical lattice constants are listed in table 1. Clearly, the theoretical lattice constants for  $\text{Fe}_3\text{Al}$  and  $\text{Fe}_2\text{VAl}$  are in rather good agreement with the corresponding experimental values. The theoretical lattice constant is only 1.5% too small for  $\text{Fe}_3\text{Al}$  and 1.4% too small for  $\text{Fe}_2\text{VAl}$ . The theoretical spin magnetic moments in  $\text{Fe}_3\text{Al}$  also agree well with those measured by neutron scattering [10] (see table 1). The electronic structure of  $\text{Fe}_3\text{Al}$  has been calculated before both nonselfconsistently [11] and selfconsistently [12]. Our theoretical magnetic moments are in good agreement with the previous selfconsistent calculations [12]. One question that has been addressed by several experimentalists [1, 8, 13] is whether V atoms go to the Fe(I) sites or to the Fe(II) in the  $(\text{Fe}_{1-x}\text{V}_x)_3\text{Al}$  alloys. Our total energy calculations (see table 1 and figure 2(b)) show that the Fe(I) site is energetically more favourable for V substitution than the Fe(II) by 0.26 eV per V atom. Furthermore, because  $\text{FeVFeAl}$  is predicted to be magnetic whilst  $\text{Fe}_2\text{VAl}$  is not, the nonmagnetic behaviour observed [8, 1] in  $\text{Fe}_2\text{VAl}$  points to the replacement of Fe(I) by V.

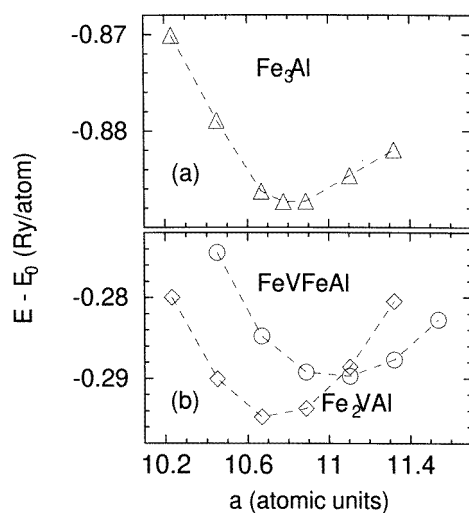


**Figure 2.** Total energy ( $E - E_0$ ) as a function of lattice constant ( $a$ ) for  $\text{Fe}_3\text{Al}$  (a),  $\text{Fe}_2\text{VAl}$  (diamonds) (b) and  $\text{FeVFeAl}$  (circles) (b).  $E_0$  is  $-1865$  Ryd/atom for panel (a) and  $-2026$  Ryd/atom for panel (b). The dashed curves are guides to the eye only.

We also performed electronic structure and total energy calculations for nonmagnetic  $\text{Fe}_2\text{VAl}$  using the highly accurate all-electron full-potential linear augmented plane wave (FLAPW) method [14]. To determine theoretically the lattice constant, the calculations were carried out for several lattice constants. The muffin-tin sphere radii used are 2.35 a.u. for Al and 2.1 a.u. for Fe and V. The number of special  $k$ -points used in the Brillouin zone integration [15] is 182 and the number of augmented plane waves (PW) included is about 90 PW/atom. The calculated lattice constant is 1.2% smaller than the experimental value but is in good agreement with the LMTO results.

We then calculate selfconsistently the electronic structure of  $\text{Fe}_2\text{VAl}$  at the experimental lattice constant. In this calculation, the nearly touching muffin-tin sphere radii (2.4 a.u. for Al and V, 2.3 a.u. for Fe) were used. Note that the results of the FLAPW calculations do not depend on the muffin-tin sphere radii used. The calculated electronic energy bands along the high-symmetry lines in the fcc Brillouin zone are shown in figure 3. The corresponding density of states spectra are displayed in figure 4. These density of states spectra were

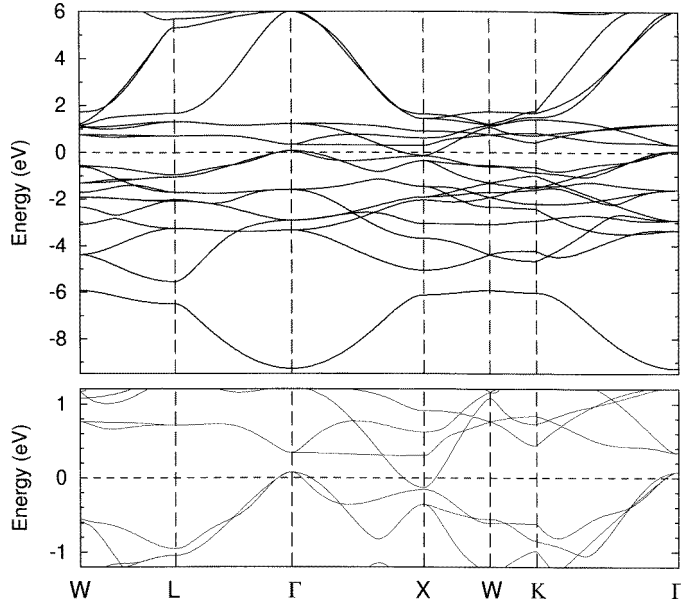


**Figure 3.**  $L2_1$   $\text{Fe}_2\text{VAI}$  energy bands along the high-symmetry lines in the fcc Brillouin zone. The Fermi level is at 0 eV.

**Table 1.** Theoretical lattice constant ( $a$ ), bulk modulus ( $B$ ), total energy ( $E$ ), density of states at the Fermi level ( $N(E_F)$ ) and spin magnetic moments ( $m$ ) in  $\text{Fe}_3\text{Al}$ ,  $\text{Fe}_2\text{VAI}$  and  $\text{FeVFeAl}$ .  $N(E_F)$  is in units of states/spin  $\text{Ryd}^{-1}/\text{atom}$  and  $E$  is in units of  $\text{Ryd}/\text{cell}$ . Experimental lattice constant and spin magnetic moments are also listed for comparison (values in brackets).

System	$a$ (au)	$B$ (Mbar)	$E$	$N(E_F)$	$m^{\text{FeI}}(\mu_B)$	$m^{\text{FeII}}(\mu_B)$	$m^{\text{V}}(\mu_B)$	$m^{\text{Al}}(\mu_B)$
$\text{Fe}_2\text{VAI}$	10.74 (10.89 <sup>a</sup> )	2.40	-7461.179	0.54		0.0	0.0	0.0
$\text{FeVFeAl}$	11.03	1.63	-7461.160	3.89 (↑) 7.70 (↓)	1.83	2.01	-0.24	-0.06
$\text{Fe}_3\text{Al}$	10.89 (10.94 <sup>a</sup> )	1.59	-8107.549	2.52 (↑) 6.83 (↓)	2.34 (2.18 <sup>b</sup> )	1.89 (1.50 <sup>b</sup> )		-0.14

<sup>a</sup>Measured by Y Nishino *et al* (1997) [1].

<sup>b</sup>Measured by S J Pickart and R Nathans (1961) [10].

calculated by using the analytic tetrahedron method [7] with 195  $k$ -points. The valence charge densities on the (110) plane are plotted in figure 5 and the Fermi surface is plotted in figure 6. The corresponding LMTO band structure and density of states are very similar and thus, are not shown here. Broadly speaking, the electronic structure of  $\text{Fe}_2\text{VAI}$  consists of two peaks in the density of states spectrum which are separated by a very steep pseudogap centred right at the Fermi level (see figure 4). There are twelve bands in the valence band manifold with the bandwidth of 9.3 eV (see figure 3). The lowest valence band, which is separated from the other valence bands by an energy gap of 0.4 eV, is of Al 3s character strongly hybridized with Fe and V 4s states. The upper part of the valence manifold is dominated by the Fe d bands with the bandwidth of 5.5 eV (see figure 4). There are nine Fe d dominant valence bands hybridized with Al 3p and V 3d orbitals and two V 3d-dominant bands in this region. The lower conduction bands (within 2 eV above the Fermi level) are made of strongly hybridized bands between Fe and V d orbitals. This covalent bonding

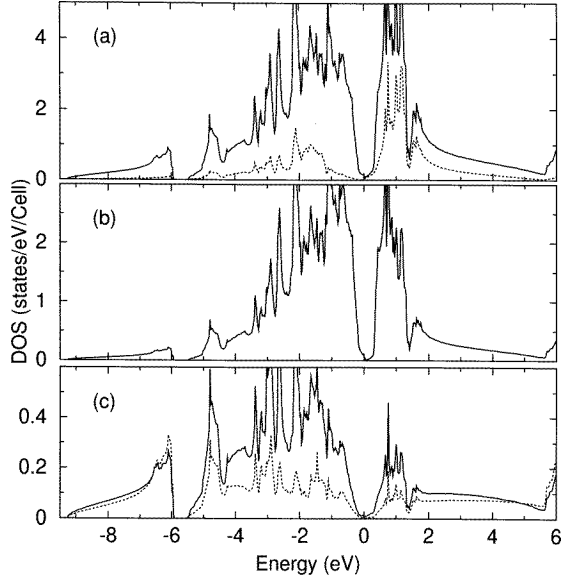


**Figure 4.**  $L2_1$   $\text{Fe}_2\text{VAl}$  total and site-decomposed densities of states (DOS). (a) Solid lines denote the total DOS; dotted lines, the DOS in the V muffin-tin sphere (MTS). (b) The DOS in the Fe MTS. (c) Solid lines denote the DOS in the interstitial region; the dotted lines, the DOS in the Al MTS. The Fermi level is at 0 eV.

between the Fe and V atoms can be clearly seen from figure 5(b).

Remarkably, the theoretical band structure predicts that  $\text{Fe}_2\text{VAl}$  is a semimetal and its Fermi surface consists of three small hole pockets centred at the  $\Gamma$  point and one small electron pocket at the X point (see figures 3 and 6). The three hole pockets come from the Fe 3d-dominant bands ( $t_{2g}$  character) whilst the electron pocket is of mainly V 3d- $e_g$  character. The density of states at the Fermi level for  $\text{Fe}_2\text{VAl}$  is about an order of magnitude smaller than that of  $\text{Fe}_3\text{Al}$  and  $\text{FeVFeAl}$  (see table 1). The electronic specific heat coefficient  $\gamma$  can be derived from the density of states at the Fermi level  $N(E_F)$  using

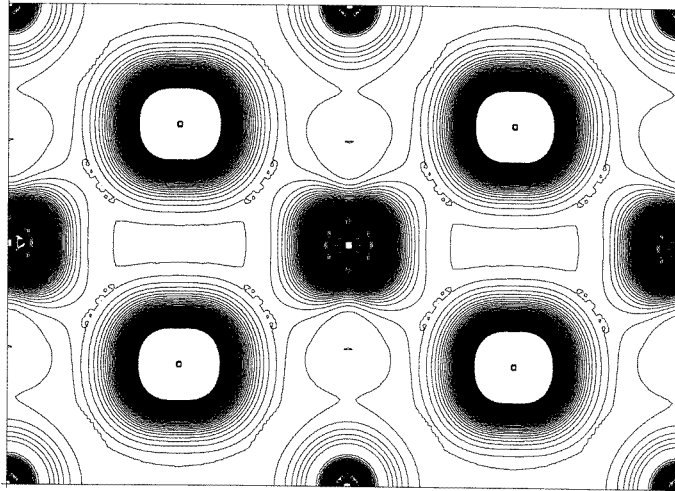
$$\gamma = \frac{2\pi^2}{3} k_B^2 N(E_F) (1 + \lambda_{ep} + \lambda_{sf}) \quad (1)$$

where  $k_B$  is the Boltzmann constant and  $\lambda_{ep}$  and  $\lambda_{sf}$  are, respectively, electron-phonon coupling and spin-fluctuation enhancements. Therefore, the bare band electronic specific heat coefficient ( $\lambda_{sf} = \lambda_{ep} = 0$ ) is only  $0.69 \text{ mJ mol}^{-1} \text{ K}^{-2}$ , about 20 times smaller than the experimental value [1] of  $14 \text{ mJ mol}^{-1} \text{ K}^{-2}$ . This large mass enhancement in  $\text{Fe}_2\text{VAl}$  appears to be in the same order of magnitude as that found in some f-electron heavy-fermion compounds [16]. Note that the gigantic mass enhancement of two to three orders of magnitude observed in the heavy-fermion compounds refers to the ratio of the observed mass to the bare electron mass (not the bare band electron mass) [16].

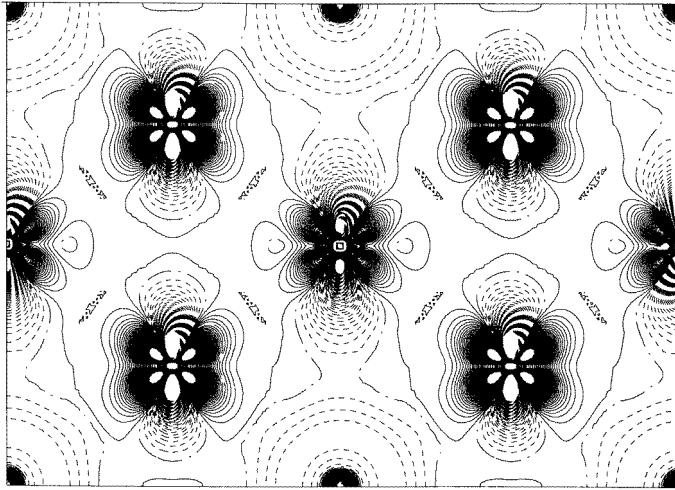
To gain insight into the origins of this large mass enhancement, let us evaluate the electron-phonon coupling parameter  $\lambda_{ep}$  within the so-called local rigid muffin-tin approximation (LRMTA) due to Gaspari and Gyorffy [18]. We may write

$$\lambda = \sum_i \frac{\eta_i}{M_i \langle \omega_i^2 \rangle}. \quad (2)$$

Using the LMTO electronic structure parameters, we estimated the electronic parameter  $\eta_i$



(a)



(b)

**Figure 5.** (a)  $L2_1$   $\text{Fe}_2\text{VAI}$  valence charge densities on the (110) plane. (b) The differences between the valence charge densities and those obtained by a superposition of the free atom charge densities. The contour step is  $0.04 \text{ e } \text{\AA}^{-3}$  for (a) and  $0.02 \text{ e } \text{\AA}^{-3}$  for (b). In (b), the dashed curves denote negative contour levels and the dashed-dot contour is set at 0. The atoms at the four corners and also at the centres of the upper and lower edges are the Al atoms. See figure 1 for the positions of the other atoms.

for all the atoms in  $\text{Fe}_2\text{VAI}$ , and we found  $\eta = 0.0036, 0.087, 1.52 \text{ eV } \text{\AA}^{-2}$ , respectively, for Al, V and Fe. Neglecting the small Al contribution and replacing [19]  $\langle \omega_i^2 \rangle$  by  $(1/2)\Theta_D^2$ , we obtained a  $\lambda_{ep}$  value of 0.53 by using the experimental Debye temperatures ( $\Theta_D$ ) for V and Fe [20]. This clearly suggests that the electron-phonon coupling contribution to the mass enhancement is of minor importance and that most of the mass enhancement is due to the spin-fluctuations in  $\text{Fe}_2\text{VAI}$ . This theoretical finding can be tested by the low-temperature magnetic susceptibility measurements. The bare band Pauli susceptibility

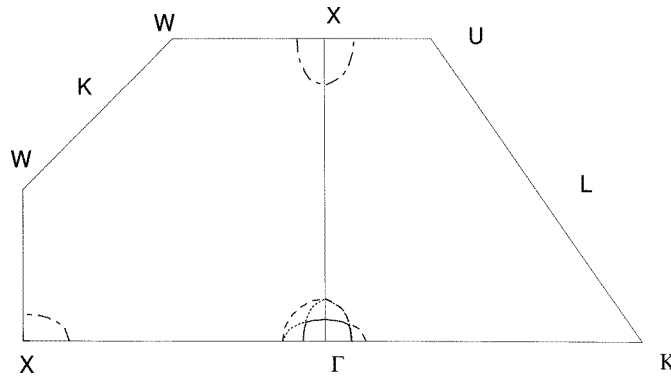


**Figure 6.**  $L2_1$   $Fe_2VAI$  Fermi surface. The solid curve denotes the hole pocket due to band 10; the dotted curve, the hole pocket due to band 11; the dashed curve, the hole pocket due to band 12; the dash-dotted curve, the electron pocket due to band 13.

should be enhanced by about the same amount as that of the electronic specific heat coefficient. It should be pointed out that the above discussion on the mass enhancement implies that the predicted and observed Fermi surface were similar. Thus, another possibility of the enhanced observed specific heat compared with the predicted bare band specific heat could be that the actual Fermi surface had a much larger area than the calculated Fermi surface (figure 6).

The theoretical electronic structure obtained here and also the observed semiconductor-like resistivity [1] in  $Fe_2VAI$  are reminiscent of  $FeSi$  which has been classified as the only d electron system among the family of rare earth ‘strongly correlated’ or ‘Kondo’ insulators [17]. However, unlike  $Fe_2VAI$  which is predicted here to be a semimetal with only a sharp pseudogap at the Fermi level, previous LSDA calculations predicted that  $FeSi$  is a nonmagnetic narrow-gap semiconductor [21]. The existence of the Fermi surface in  $Fe_2VAI$  appears to be consistent with the recent photoemission measurement which revealed a clear Fermi cutoff [1]. Figures 3 and 6, nevertheless, show that both the electron and hole pockets are very small, thereby giving rise to only very small electrical carrier concentrations in  $Fe_2VAI$ . The observed poor conducting behaviour at low temperatures in  $Fe_2VAI$  might then be explained by the carrier localization in the presence of impurities and disorders. Another more exciting possibility would be a gap opening caused by either ‘Kondo’ transition or spin-fluctuations in this ‘strongly correlated’ system. In this respect further de Haas–van Alphen experiments will be very useful since they not only determine the possible existence of the predicted Fermi surface (figure 6) but also reveal the nature of the electronic mass enhancement. Note that the indirect overlap between the valence band and conduction band is only 0.2 eV. It is well known that the LSDA calculations often underestimate the band gap in semiconductors although they give excellent ground state properties such as structural parameters and elastic constants. To see the possible effects of some corrections to the LSDA on the gap size, we also performed selfconsistent LMTO calculations for  $Fe_2VAI$  including the so-called generalized gradient corrections [22, 23] to the LSDA. Nevertheless, the band structure remained almost unchanged.

In conclusion, our first-principles spin-polarized electronic structure and total energy calculations predict that in the ordered  $(Fe_{0.67}V_{0.33})_3Al$  alloy, the V atoms replace the Fe(I) atoms in the parent  $DO_3$   $Fe_3Al$  compound, thus giving rise to a Heusler-type compound. Our calculations also show that the Heusler-type  $Fe_2VAI$  is a nonmagnetic semimetal with



a narrow pseudogap at the Fermi level. Both the estimated electron–phonon coupling parameter and the calculated large Fe (V) d dominated density of states sitting immediately above and below the Fermi level (figure 4) suggest that the large mass enhancement of the electronic specific heat coefficient observed in Fe<sub>2</sub>VAl [1] is mainly due to the strong spin excitations in this compound. Further theoretical work on the magnetic fluctuations along the lines, e.g., of both Jarlborg [21] and Takahashi [24] will be very helpful. The predicted existence of the Fermi surface is consistent with the observed clear Fermi cutoff in the photoemission experiment [1], and the observed semiconductor behaviour in electrical resistivity is tentatively attributed to the existence of the very small carrier concentrations in this material. Further low-temperature magnetic susceptibility and de Haas–van Alphen measurements are needed in order to clarify the existence of the Fermi surface and the nature of the mass enhancement.

## References

- [1] Nishino Y *et al* 1997 *Phys. Rev. Lett.* **79** 1909
- [2] Andersen O K 1975 *Phys. Rev.* **12** 3060
- [3] Hohenberg P and Kohn W 1964 *Phys. Rev.* **136** B864
- [4] Kohn W and Sham L J 1965 *Phys. Rev.* **140** A1133
- [5] Vosko S H, Wilk L and Nusair M 1980 *Can. J. Phys.* **58** 1200
- [6] Koelling D D and Harmon B N 1977 *J. Phys. C: Solid State Phys.* **10** 3107
- [7] Jepsen O and Andersen O K 1971 *Solid State Commun.* **9** 1763
- [8] Popiel E *et al* 1989 *J. Less-Common Met.* **146** 127
- [9] Murnaghan F D 1944 *Proc. Natl Acad. Sci. USA* **30** 244
- [10] Pickart S J and Nathans R 1961 *Phys. Rev.* **123** 1163
- [11] Ishida S *et al* 1976 *J. Phys. Soc. Japan* **41** 1570
- [12] Eriksson O, Boring A M and Johansson B 1990 *Phys. Rev. B* **41** 11 807
- [13] Okpalugo D E, Booth J G and Faunce C A 1985 *J. Phys. F: Met. Phys.* **15** 681
- [14] Blaha P *et al* 1990 *Comput. Phys. Commun.* **42** 399
- [15] Monkhorst H J and Pack J D 1980 *Phys. Rev. B* **13** 5188
- [16] Fisk Z *et al* 1988 *Science* **239** 33
- [17] Schlesinger Z *et al* 1993 *Phys. Rev. Lett.* **71** 1748
- [18] Gaspari G D and Gyorffy B L 1972 *Phys. Rev. Lett.* **28** 801
- [19] Jarlborg T and Freeman A J 1980 *Phys. Rev. B* **22** 2332
- [20] Kittel C 1996 *Introduction to Solid State Physics* (New York: Wiley) p 126
- [21] Jarlborg T 1995 *Phys. Rev. B* **51** 11 106
- [22] Langreth D C and Mehl M J 1983 *Phys. Rev. B* **28** 1809
- [23] Hu C D and Langreth D C 1985 *Phys. Scr.* **32** 391
- [24] Takahashi Y 1997 *J. Phys.: Condens. Matter* **9** 2593